Supplementary Information (SI) for Environmental Science: Processes & Impacts.
This journal is © The Royal Society of Chemistry 2025

Supplemental Information

Insight into the interactions between microplastics and heavy metals: Adsorption performance influenced by microplastic types

Yu-liang Liao, ‡[a,b] Chun-dan Gan, ‡[a,c] Xue Zhao, [d] Xin-yue Du [a,c] and Jin-yan Yang *[a,b,c]

[a] College of Architecture and Environment, Sichuan University, Chengdu 610065, China

[b] Key Laboratory of Environment Remediation and Ecological Health (Zhejiang University), Ministry of Education, China

[c] Yibin Institute of Industrial Technology, Sichuan University Yibin Park, Yibin 644000, China

‡These authors contributed equally to this work.

*Corresponding author, Tel. (86)28-85404241, E-mail. yanyang@scu.edu.cn

24 pages; 4 texts, 1 figure, 16 tables

Text S1. Synthesis of EMPs

Fresh new plastic balls (PE, PP, PVC, or polycarbonate), plastic films (PE or PP), plastic tubes (PVC), plastic nets (PP or PS), plastic ropes (PS or polyamide), and plastic bottles (polyethylene terephthalate, PET) were purchased from the market. Plastic films and pellets were cut or crushed into different sizes using blades, pulverizers, and cutters. For soft plastics, rapid freezing with liquid nitrogen was conducted before cutting and crushing. Small plastic particles were ground after rapid freezing with liquid nitrogen. Granule, film, and fiber MPs of different sizes were obtained by sieving through sieves with apertures of 5 mm, 1 mm, 750 μm, 500 μm, 250 μm, 100 μm, and 50 μm. The quantity of plastic particles per unit mass was calculated by counting 0.01 g of different plastic particles under a stereomicroscope (Saga-sg700, Suzhou, China).

Text S2. Aging of MPs

(1) UV irradiation

A UV lamp was used to ensure consistent UV irradiation, with a day/night alternating schedule set to simulate natural sunlight. To prevent interference, an opaque sealed box with a UV lamp on top was constructed to quantitatively control the irradiation dose (UV-A: 13.6 W/m^2; UV-B: 3.0 W/m^2) received by the MPs. The ratio of UV-A to UV-B emitted by the UV lamp (OSRAM, ULTRA-VITALUX, Germany) was designed to closely mimic natural daylight, and the day/night ratio was set to 10 h/14 h. During aging, initial particles of each of the six MPs were placed in petri dishes and laid flat in the opaque sealed box for 60 d. The MPs were thoroughly mixed every 5 d to ensure uniform irradiation. In the control group, petri dishes containing MPs were placed in the same sealed box under identical conditions, but the outer surfaces of the petri dishes were covered with light-impermeable aluminum foil and kept for 60 d. After aging, the MPs were removed from the box and stored in the dark.

(2) Mechanical abrasion

To simulate the mechanical abrasion of soil particles on MPs, SiO_2 particles were utilized for physical aging. Two types of SiO_2 particles with particle sizes of 100 μm and 1000 μm were mixed and pretreated eliminate potential contaminants such as microorganisms and heavy metals, ensuring minimal external interference. Initially, SiO_2 particles were combined with a 10% HCl solution at a solid-liquid ratio of 1:5 (*w:v*) in a clean conical flask and shaken for 24 h. Following this, the SiO_2 particles were washed three times with deionized water and air-dried. The pretreated SiO_2 particles were then placed into six conical flasks, each containing one of the six types of UV-aged MPs, at a mass ratio of 1:50. The conical flasks were sealed with opaque aluminum foil and rotated at 50 rpm for 60 d to simulate mechanical abrasion. A control group was also established, where the MPs were mixed with the pretreated SiO_2 in the same manner but stored without rotation and protected from light for 60 d. After the aging process, the mixtures in the conical flasks were subjected to density separation based on the densities of the MPs using deionized water, saturated NaCl solution, or saturated NaI solution. The upper layer of the liquid was collected after centrifugation at 4000 g for 5 min and then subjected to vacuum filtration using a 50 μm filter membrane. The MPs collected on the membrane were rinsed with deionized water, dried, and stored in a sealed container for further analysis.

Text S3. Characterization of MPs

The morphology of MPs before and after the aging process were characterized by scanning electron microscope (SEM, Zeiss Sigma 300, Zeiss Inc., Jena, Germany) in the condition of an acceleration voltage of 3/5 kV and work distance with 6.1–9.6 mm. Microplastic particles were analyzed in a confocal micro-Raman spectrometer using an inVia Raman microscope (Renishaw Plc, Wotton-under-Edge, UK) equipped with a 785 nm diode laser and a 600 lines/mm diffraction grating, with a choice of 20×, 50×, or 100× objective lenses in both extended and static scanning modes at 10–50 mW laser power and 1 s CCD exposure time. Five samples per slide were randomly scanned to obtain Raman spectra, which were then compared to a library of standard spectra to determine the chemical composition of the MPs. The system calibration was performed using an in-house silicon wafer, characterized by a band at 520 cm^{-1}, before each test. Following analysis, the MPs on the slides were rinsed with ethanol and stored in Petri dishes.

Text S4. Preparation of artificial soil solution

Experiments were conducted using the reagents listed in Table S1, excluding NH_4NO_3, and deionized water to prepare reserve solutions (×100 fold). Before each adsorption experiment, the artificial soil solution was prepared by diluting the stock solution stored at 4°C, with NH_4NO_3 added separately in proportion to the dilution. The pH of the soil solution was then adjusted to 6.4 using NaOH and HNO_3. This formulation of the artificial soil solution was designed to exclude highly variable factors such as humic acid, soil colloids, and microorganisms, to focus on elucidating the adsorption-desorption mechanisms of MPs and HMs. Consequently, it does not fully simulate the solutes and suspended matter typically found in natural soil solutions.

Text S5. Modeling

(1) Kinetic models

The pseudo-first order kinetic model can be expressed in equation (2):

$$Q_t = Q_{e,1}\left(1-e^{-k_1 t}\right) \tag{2}$$

where Q_t (mg/g) is the adsorbed amount at time t, $Q_{e,1}$ (mg/g) is the pseudo-first-order kinetic adsorption capacity at adsorption equilibrium, and k_1 (h^{-1}) is the adsorption rate under pseudo-first-order kinetics.

The pseudo second-order kinetic model and its linear variant can be expressed in equation (3) and (4), respectively:

$$Q_t = \frac{k_2 Q_{e,2}^2 t}{1 + k_2 Q_{e,2} t} \tag{3}$$

$$\frac{t}{Q_t} = \frac{1}{k_2 Q_{e,2}^2} + \frac{t}{Q_{e,2}} \tag{4}$$

where Q_t (mg/g) is the adsorbed amount at time t, $Q_{e,2}$ (mg/g) is the pseudo-second-order kinetic adsorption capacity at adsorption equilibrium, and k_2 (g/mg·h) is the adsorption rate under pseudo-first-order kinetics. k_2 and $Q_{e,2}$ can be computed from the slope ($1/Qe$) and intercept of the linear fit of t/Qt to t using Equation (4).

The Elovich model, a modification of the Elovich equation, is suitable for describing non-single-reaction adsorption processes that may involve chemical reactions with multiple factors and steps. It is commonly used to study medium transfer processes in soils. The external diffusion model and the intraparticle diffusion model describe the diffusive changes in concentration gradient between the adsorption interface and the medium, and are often employed to identify the rate-limiting step controlling the adsorption rate. The mathematical forms of these three models can be expressed in equations (5), (6) and (7):

$$Q_t = a + b\ln(t) \quad (5)$$

$$\ln\frac{C_t}{C_0} = -k_3 t \quad (6)$$

$$Q_t = k_p t^{0.5} + S \quad (7)$$

where Q_t (mg/g) is the adsorbed amount at time t, a (mg/g) and b (mg/g-min) are the Elovich coefficients, C_t (mg/L) is the amount of HM in solution, C_0 (mg/L) is the initial concentration of the HM in solution, k_3 (h^{-1}) is the coefficient of the external diffusion model, k_p ($mg/g \cdot h^{0.5}$) is the coefficient of the intraparticle diffusion model, and S (mg/g) is the constant of the intraparticle diffusion model.

(2) Isotherm models

The results of isothermal adsorption experiments were fitted using Langmuir, Freundlich and Henry adsorption isotherms, respectively. The mathematical forms of the above three models can be represented by equations (8), (9) and (10), respectively:

$$Q_e = \frac{Q_m K_L C_e}{1 + K_L C_e} \tag{8}$$

$$Q_e = K_F C_e^{1/n} \tag{9}$$

$$Q_e = K_d C_e \tag{10}$$

where Q_e (mg/g) is the adsorption capacity at the adsorption equilibrium state, Q_m (mg/g) is the maximum adsorption capacity, C_e (mg/L) is the HM concentration at the adsorption equilibrium state, K_L (L/g) is the Langmuirc modeling constant with respect to t, which denotes the strength of attachment and affinity, K_F (L/g) is the Freundlich constant related to the sorption capacity, n is heterogeneity factor, and K_d (L/g) is the partition coefficient of the adsorbent.

The R_L values for the Langmuir isothermal adsorption model were calculated using equation (11):

$$R_L = \frac{1}{1 + K_L C_e} \tag{11}$$

where the value of R_L can be used to determine the thermodynamic type of the adsorption process: irreversible adsorption process when R_L=0; favorable adsorption process when 0<R_L<1; linear adsorption process when R_L=1; and unfavorable adsorption process when R_L>1.

The adsorption capacity of different MPs for HMs was calculated for each adsorption curve using equation (12):

$$Q_e = \frac{V(C_0 - C_e)}{m} \tag{12}$$

where Q_e (mg/g) is the adsorption capacity in the adsorption equilibrium state, V (L) is the volume of the adsorption solution, C_0 (mg/L) is the concentration of HM in the initial state, C_e (mg/L) is the concentration of HMs in the adsorption equilibrium state, and m (g) is the mass of MPs.

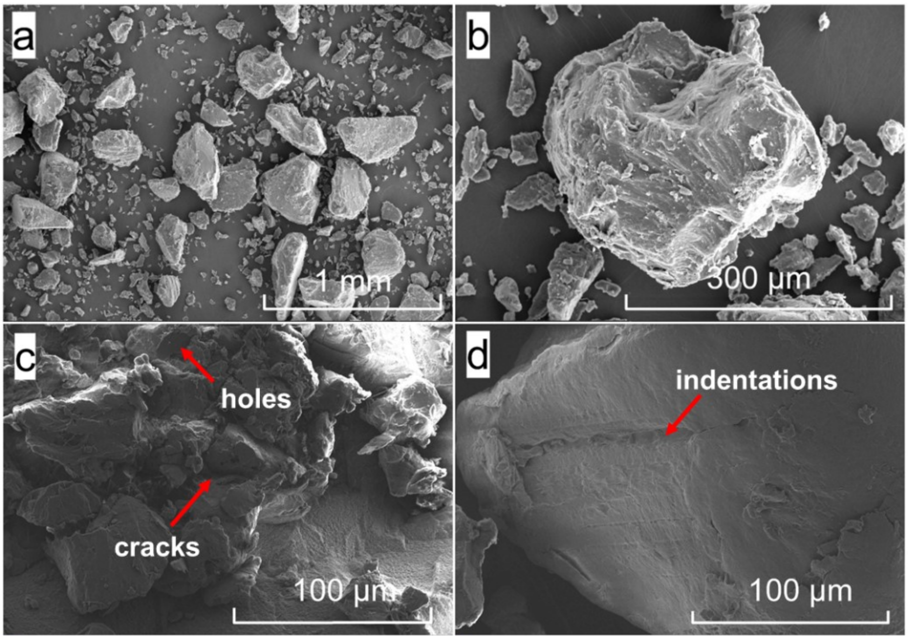

Fig. S1. SEM images of (a, b) initial and (c, d) aged PLA.

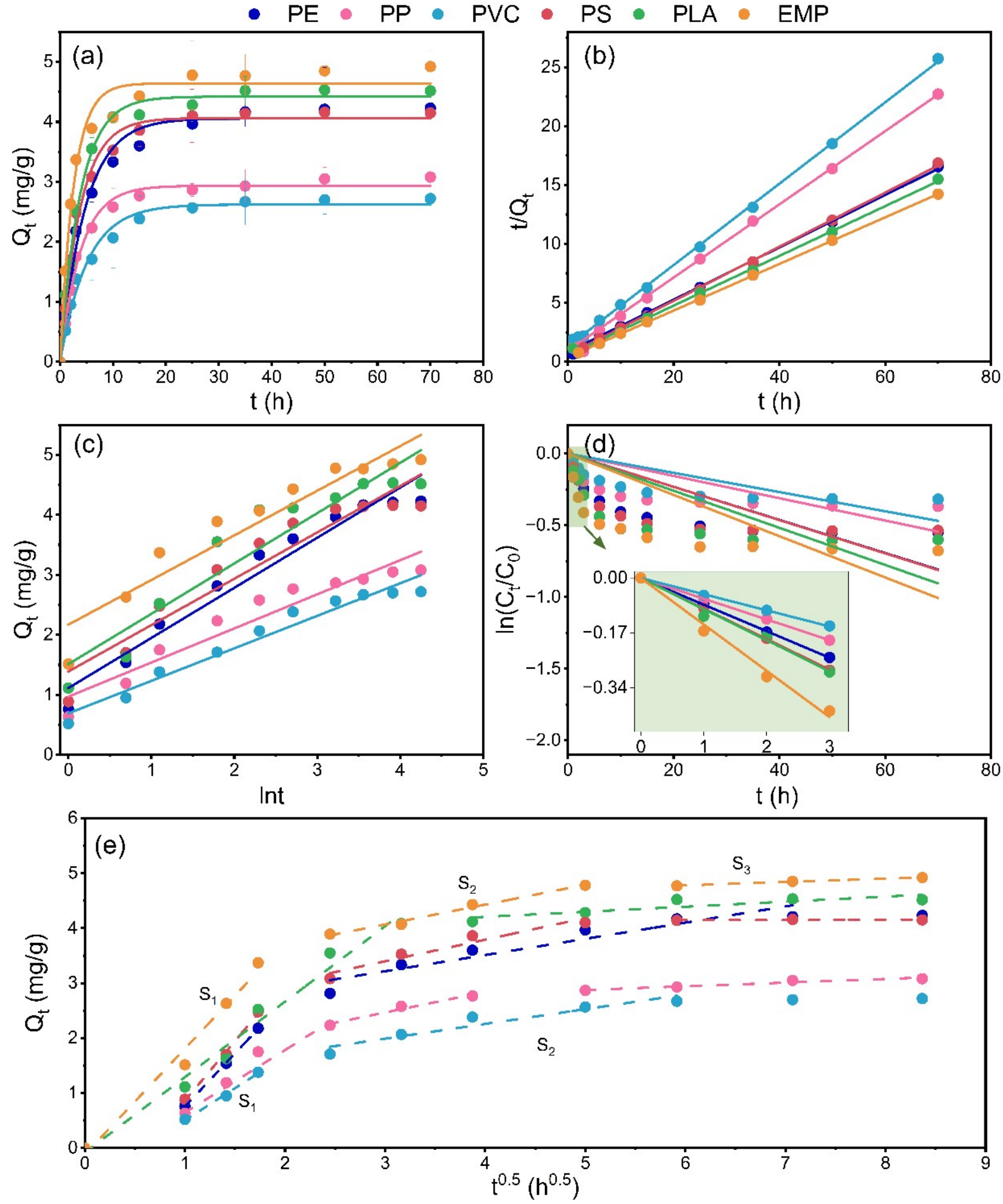

Fig. S2. The kinetics of high concentration Cd adsorption on microplastics. (a) Pseudo-first-order-kinetic, (b) Pseudo-second-order-kinetic, (c) Elovich model, (d) external diffusion model, and (e) intraparticle diffusion model.

156 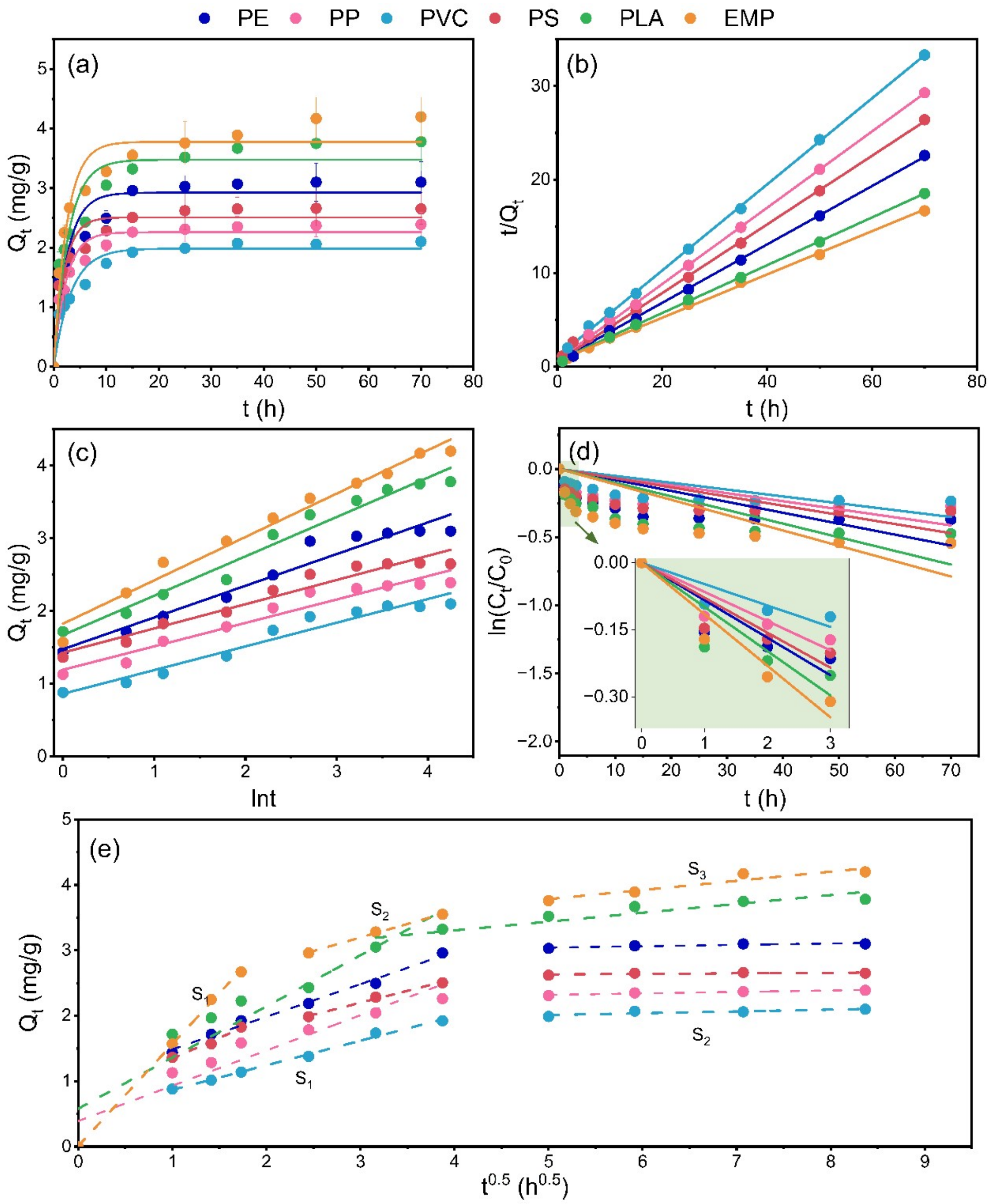

157 **Fig. S3.** The kinetics of high concentration Cr adsorption on microplastics. (a)

158 Pseudo-first-order-kinetic, (b) Pseudo-second-order-kinetic, (c) Elovich model, (d)

159 external diffusion model, and (e) intraparticle diffusion model.

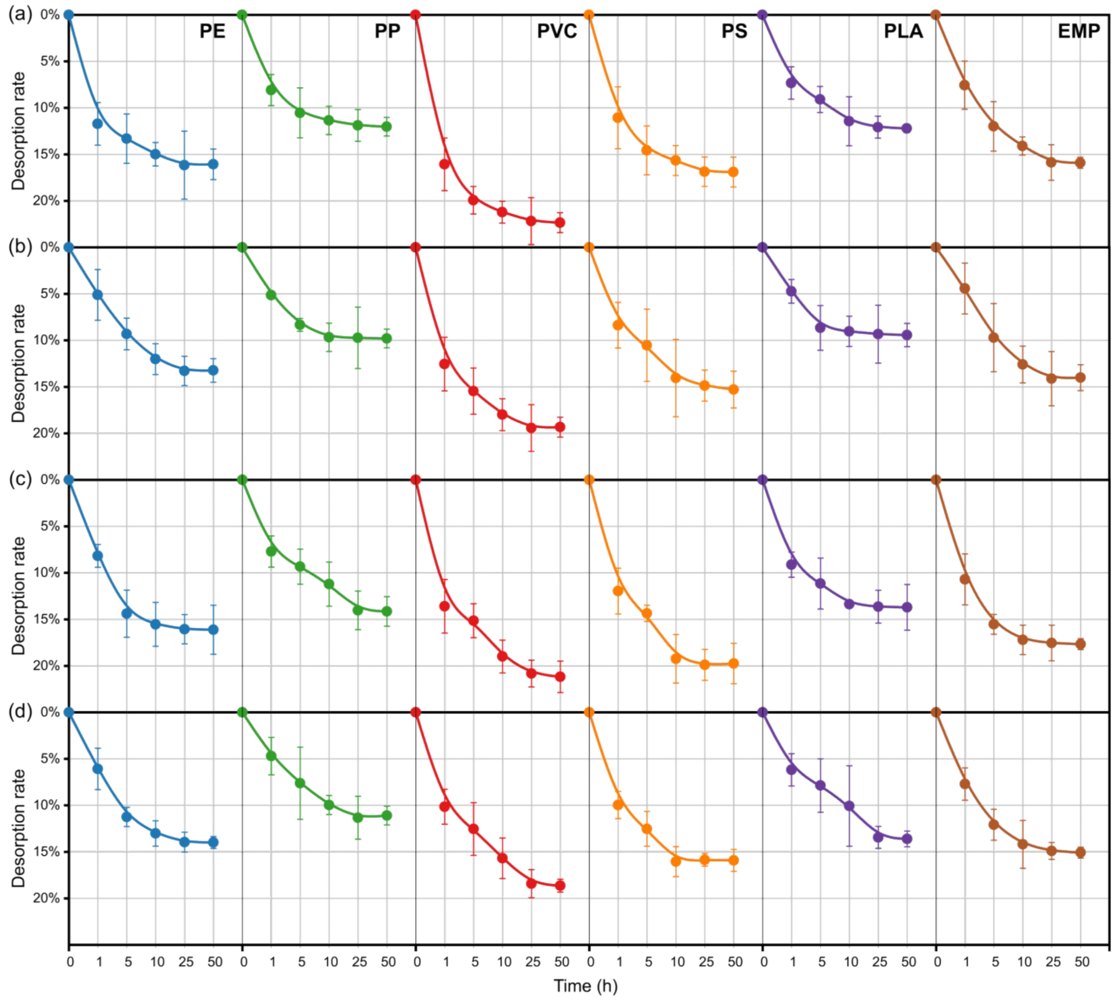

Fig. S4. Desorption of heavy metals from microplastics in artificial soil solutions: (a) Cd-loaded at 10 mg/L, (b) Cd-loaded at 100 mg/L, (c) Cr-loaded at 10 mg/L, (d) Cr-loaded at 100 mg/L.

Table S1 The recipe for artificial soil solution

Chemical composition	Dose (mg/L)	Ion concentration (μM)	
		Cations	Anions
$CaCl_2 \cdot 2H_2O$	36.76	250 Ca^{2+}	500 Cl^-
KNO_3	15.15	150 K^+	150 NO_3^-
Na_2SO_4	8.522	120 Na^+	60 SO_4^{2-}
NH_4NO_3	26.41	330 NH_4^+	330 NO_3^-
$MgSO_4 \cdot 7H_2O$	24.65	100 Mg^{2+}	100 SO_4^{2-}

Table S2 Kinetic parameters of Pseudo-first-order-kinetic and Pseudo-second-order-kinetic model for the adsorption of low concentration Cd on microplastics

MPs	Pseudo-first-order-kinetic			Pseudo-second-order-kinetic		
	K_1 (h^{-1})	$Q_{e,1}$ (mg/g)	R^2	K_2 (g/mg·h)	$Q_{e,2}$ (mg/g)	R^2
PE	0.22±0.0113	0.46±0.0231	0.994	2.13±0.3437	0.48±0.0356	0.997
PP	0.20±0.3082	0.43±0.3082	0.993	1.23±0.2770	0.46±0.0518	0.992
PVC	0.18±0.0117	0.23±0.0167	0.993	0.27±0.0386	0.21±0.0312	0.993
PS	0.26±0.0102	0.49±0.0184	0.997	3.44±0.5430	0.54±0.0285	0.998
PLA	0.20±0.3103	0.77±0.3103	0.968	4.95±0.2303	0.76±0.0181	0.999
EMP	0.25±0.1204	0.96±0.1317	0.986	24.27±2.217	1.06±0.0372	0.999

Table S3 Kinetic parameters of Elovich model and external diffusion model for the adsorption of low concentration Cd on microplastics

MPs	Elovich			External diffusion	
	a (mg/g)	β (g/mg·min)	R^2	K_3 (h^{-1})	R^2
PE	1.39±0.5234	2.76±0.3454	0.876	-0.0071±0.0000516	0.884
PP	1.02±0.3587	2.97±0.3725	0.876	-0.0056±0.0000184	0.978
PVC	0.54±0.1452	4.51±0.4594	0.915	-0.0047±0.0000435	0.773
PS	2.13±0.9316	2.72±0.3518	0.997	-0.0074±0.0000364	0.949
PLA	2.02±0.3139	2.11±0.1056	0.978	-0.0067±0.0000515	0.845
EMP	4.11±1.3835	1.40±0.1390	0.918	-0.0107±0.0000519	0.945

171 **Table S4** Kinetic parameters of intrapaticle diffusion model for the adsorption of low concentration Cd on microplastics

MPs	$K_{p,1}$ (mg/g·h$^{0.5}$)	S_1 (mg/g)	R^2	$K_{p,2}$ (mg/g·h$^{0.5}$)	S_2 (mg/g)	R^2	$K_{p,3}$ (mg/g·h$^{0.5}$)	S_3 (mg/g)	R^2
PE	0.68±0.086	-0.35±0.15	0.953	0.0032±0.0069	1.52±0.04	0.807	-	-	-
PP	0.66±0.046	-0.45±0.079	0.986	0.03±0.012	1.33±0.07	0.513	-	-	-
PVC	0.38±0.021	-0.25±0.037	0.991	0.029±0.0025	0.79±0.015	0.964	-	-	-
PS	0.94±0.079	-0.54±0.11	0.986	0.22±0.016	0.99±0.053	0.989	0.0081±0.0022	1.92±0.014	0.949
PLA	0.83±0.071	-0.21±0.10	0.985	0.41±0.036	0.52±0.12	0.985	0.064±0.014	2.01±0.095	0.863
EMP	1.86±0.955	-1.01±0.955	0.978	0.60±0.017	1.25±0.054	0.998	0.040±0.011	3.6±0.071	0.811

Table S5 Kinetic parameters of Pseudo-first-order-kinetic and Pseudo-second-order-kinetic model for the adsorption of high concentration Cd on microplastics

MPs	Pseudo-first-order-kinetic			Pseudo-second-order-kinetic		
	K_1 (h^{-1})	$Q_{e,1}$ (mg/g)	R^2	K_2 (g/mg·h)	$Q_{e,2}$ (mg/g)	R^2
PE	0.21±0.3024	4.06±0.3024	0.984	24.73±1.9691	4.50±0.0449	0.999
PP	0.26±0.2762	2.94±0.2762	0.990	11.12±0.8719	3.22±0.0278	0.999
PVC	0.20±0.3153	2.62±0.3153	0.984	6.45±0.4251	2.89±0.0274	0.999
PS	0.26±0.2736	4.06±0.2736	0.990	32.67±4.3724	4.36±0.0533	0.999
PLA	0.26±0.2735	4.42±0.2735	0.993	41.72±5.4879	4.73±0.0572	0.999
EMP	0.39±0.2313	4.64±0.2313	0.975	66.13±5.0900	5.05±0.0267	0.999

Table S6 Kinetic parameters of Elovich model and external diffusion model for the adsorption of high concentration Cd on microplastics

MPs	Elovich			External diffusion	
	α (mg/g)	β (g/mg·min)	R^2	K_3 (h^{-1})	R^2
PE	3.17±0.7277	1.20±0.0915	0.950	0.082±0.0006500	0.999
PP	3.13±1.0794	1.76±0.1816	0.912	0.064±0.0003037	0.999
PVC	1.94±0.4152	1.84±0.1334	0.955	0.050±0.0003356	0.999
PS	4.66±1.7994	1.29±0.1457	0.897	0.094±0.0009624	0.999
PLA	5.08±2.1513	1.19±0.1470	0.879	0.096±0.0009520	0.984
EMP	13.73±7.118	1.34±0.1556	0.892	0.146±0.001263	0.988

Table S7 Kinetic parameters of intrapaticle diffusion model for the adsorption of high concentration Cd on microplastics

MPs	$K_{p,1}$ (mg/g·h$^{0.5}$)	S_1 (mg/g)	R^2	$K_{p,2}$ (mg/g·h$^{0.5}$)	S_2 (mg/g)	R^2	$K_{p,3}$ (mg/g·h$^{0.5}$)	S_3 (mg/g)	R^2
PE	1.93±0.038	-1.18±0.054	0.999	0.30±0.051	2.33±0.25	0.869	-	-	-
PP	1.14±0.024	-0.49±0.012	0.979	0.37±0.059	1.34±0.17	0.942	0.067±0.012	2.54±0.084	0.908
PVC	1.17±0.028	-0.66±0.031	0.989	0.27±0.043	1.18±0.10	0.879	-	-	-
PS	2.17±0.135	-1.13±0.191	0.992	0.39±0.070	2.22±0.26	0.910	0.0038±0.0072	4.12±0.052	0.222
PLA	1.37±0.024	-0.083±0.19	0.974	0.09±0.102	3.84±0.54	0.661	-	-	-
EMP	1.93±0.19	-0.12±0.23	0.971	0.36±0.030	2.98±0.11	0.980	0.06±0.0043	4.41±0.031	0.990

Table S8 Kinetic parameters of Pseudo-first-order-kinetic and Pseudo-second-order-kinetic model for the adsorption of low concentration Cr on microplastics

MPs	Pseudo-first-order-kinetic			Pseudo-second-order-kinetic		
	K_1 (h^{-1})	$Q_{e,1}$ (mg/g)	R^2	K_2 (g/mg·h)	$Q_{e,2}$ (mg/g)	R^2
PE	0.21±0.0114	0.89±0.0131	0.993	0.25±0.0273	0.98±0.0147	0.998
PP	0.23±0.0177	0.67±0.0135	0.988	0.11±0.0170	0.74±0.0154	0.996
PVC	0.17±0.0105	0.50±0.0083	0.993	0.034±0.0041	0.57±0.0153	0.994
PS	0.20±0.0113	0.80±0.0117	0.994	0.20±0.0232	0.87±0.0129	0.998
PLA	0.27±0.0099	0.83±0.0732	0.997	0.30±0.0528	0.87±0.0123	0.998
EMP	0.27±0.0141	0.94±0.0122	0.994	0.41±0.0666	1.00±0.0145	0.998

Table S9 Kinetic parameters of Elovich model and external diffusion model for the adsorption of low concentration Cr on microplastics

MPs	Elovich			External diffusion	
	α (mg/g)	β (g/mg·min)	R^2	K_3 (h^{-1})	R^2
PE	0.64±0.1935	5.31±0.5517	0.914	0.012±0.0009072	0.940
PP	0.56±0.1911	7.25±0.7927	0.903	0.0096±0.001157	0.864
PVC	0.26±0.0513	8.83±0.6942	0.947	0.0060±0.000332	0.969
PS	0.61±0.1814	6.10±0.5940	0.922	0.014±0.001239	0.838
PLA	1.13±0.5342	6.55±0.9363	0.844	0.013±0.001262	0.904
EMP	1.14±0.4967	5.68±0.7377	0.870	0.015±0.001377	0.918

Table S10 Kinetic parameters of intrapaticle diffusion model for the adsorption of low concentration Cr on microplastics

MPs	$K_{p,1}$ (mg/g·h$^{0.5}$)	S_1 (mg/g)	R^2	$K_{p,2}$ (mg/g·h$^{0.5}$)	S_2 (mg/g)	R^2	$K_{p,3}$ (mg/g·h$^{0.5}$)	S_3 (mg/g)	R^2
PE	0.27±0.036	-0.048±0.055	0.933	0.058±0.014	0.59±0.057	0.892	0.015±0.0023	0.80±0.015	0.934
PP	0.26±0.052	-0.13±0.089	0.892	0.11±0.032	0.24±0.10	0.828	0.016±0.0044	0.58±0.029	0.798
PVC	0.20±0.028	-0.14±0.040	0.961	0.081±0.006	0.14±0.019	0.989	0.014±0.0066	0.41±0.044	0.554
PS	0.34±0.034	-0.19±0.048	0.980	0.16±0.051	0.16±0.160	0.808	0.005±0.0020	0.78±0.013	0.640
PLA	0.28±0.026	-0.034±0.04	0.967	0.0097±0.0018	0.76±0.011	0.842	-	-	-
EMP	0.33±0.033	-0.048±0.051	0.960	0.022±0.0062	0.80±0.036	0.691	-	-	-

Table S11 Kinetic parameters of Pseudo-first-order-kinetic and Pseudo-second-order-kinetic model for the adsorption of high concentration Cr on microplastics

MPs	Pseudo-first-order-kinetic			Pseudo-second-order-kinetic		
	K_1 (h^{-1})	$Q_{e,1}$ (mg/g)	R^2	K_2 (g/mg·h)	$Q_{e,2}$ (mg/g)	R^2
PE	0.40±0.0701	2.92±0.1242	0.916	18.37±2.6901	3.25±0.0315	0.999
PP	0.43±0.0631	2.33±0.0724	0.943	8.97±0.8127	2.44±0.0137	0.999
PVC	0.30±0.0493	2.00±0.0762	0.931	4.45±0.4757	2.28±0.0203	0.999
PS	0.50±0.0835	2.53±0.0871	0.927	14.78±2.0083	2.71±0.0209	0.999
PLA	0.36±0.0718	3.54±0.1585	0.898	25.17±2.9528	3.93±0.0391	0.999
EMP	0.41±0.0649	3.87±0.1367	0.936	31.88±4.6059	4.34±0.0627	0.999

192 **Table S12** Kinetic parameters of Elovich model and external diffusion model for the

193 adsorption of high concentration Cr on microplastics

MPs	Elovich			External diffusion	
	α (mg/g)	β (g/mg·min)	R^2	K_3 (h^{-1})	R^2
PE	12.89±5.1892	2.29±0.1867	0.943	0.084±0.008072	0.750
PP	13.03±5.9411	3.10±0.2709	0.936	0.065±0.009527	0.789
PVC	4.60±1.5489	3.07±0.2452	0.946	0.048±0.006532	0.709
PS	24.23±11.5914	3.00±0.2480	0.942	0.078±0.004646	0.752
PLA	11.82±3.3425	1.85±0.1127	0.968	0.099±0.001356	0.727
EMP	12.73±3.1767	1.68±0.0907	0.975	0.12±0.001301	0.911

Table S13 Kinetic parameters of intrapaticle diffusion model for the adsorption of high concentration Cr on microplastics

MPs	$K_{p,1}$ (mg/g·h$^{0.5}$)	S_1 (mg/g)	R^2	$K_{p,2}$ (mg/g·h$^{0.5}$)	S_2 (mg/g)	R^2	$K_{p,3}$ (mg/g·h$^{0.5}$)	S_3 (mg/g)	R^2
PE	0.50±0.038	0.99±0.054	0.987	0.021±0.011	2.91±0.16	0.731	-	-	-
PP	0.54±0.044	0.39±0.022	0.882	0.023±0.010	2.25±0.25	0.901	-	-	-
PVC	0.38±0.018	0.49±0.057	0.993	0.028±0.015	1.94±0.14	0.617	-	-	-
PS	0.63±0.085	0.72±0.096	0.964	0.37±0.031	1.13±0.10	0.986	0.0082±0.0061	2.62±0.041	0.221
PLA	0.78±0.101	0.58±0.074	0.879	0.13±0.021	2.81±0.36	0.835	-	-	-
EMP	1.63±0.029	0.0092±0.036	0.999	0.41±0.028	2.08±0.22	0.995	0.14±0.032	3.17±0.22	0.855

Table S14 Fitting results of Cd onto MPs by adsorption isotherms models

MPs	Henry model		Langmuir model			Freundlich model		
	K_d (L/g)	R^2	Q_m (mg/g)	R_L	R^2	K_F (L/g)	n	R^2
PE	0.058±0.0073	0.840	5.79±0.242	0.046	0.993	0.77±0.0288	0.51±0.0248	0.977
PP	0.037±0.0067	0.707	4.29±0.0858	0.047	0.959	0.75±0.0272	0.51±0.0251	0.969
PVC	0.037±0.0048	0.828	4.49±0.233	0.022	0.955	0.66±0.0198	0.53±0.0279	0.914
PS	0.054±0.0099	0.699	5.50±0.175	0.053	0.982	0.73±0.0398	0.47±0.0377	0.940
PLA	0.058±0.011	0.694	5.51±0.208	0.12	0.957	1.24±0.031	0.25±0.0109	0.983
EMP	0.059±0.0152	0.542	6.33±0.131	0.96	0.965	1.10±0.022	0.94±0.0342	0.987

199 **Table S15** Fitting results of Cr onto MPs by adsorption isotherms models

MPs	Henry model		Langmuir model			Freundlich model		
	K_d (L/g)	R^2	Q_m (mg/g)	R_L	R^2	K_F (L/g)	n	R^2
PE	0.031±0.0052	0.738	3.26±0.160	0.14	0.947	1.02±0.0260	0.27±0.0165	0.964
PP	0.020±0.0050	0.541	2.58±0.131	0.19	0.984	1.08±0.0203	0.17±0.0117	0.953
PVC	0.017±0.0039	0.596	2.49±0.083	0.09	0.976	0.85±0.0624	0.27±0.0445	0.777
PS	0.021±0.0053	0.546	2.89±0.017	0.22	0.998	1.10±0.0312	0.19±0.0121	0.913
PLA	0.047±0.0078	0.751	4.20±0.134	0.09	0.994	1.07±0.034	0.31±0.0207	0.962
EMP	0.044±0.0098	0.613	5.07±0.008	0.36	0.993	1.27±0.034	0.22±0.0191	0.938

Table S16 The heavy metals load on different loaded microplastics

	Loaded amount (mg/g)					
	PE	PP	PVC	PS	PLA	EMP
Cd_{10}	0.91±0.065	0.77±0.12	0.53±0.08	0.92±0.013	0.86±0.056	0.98±0.02
Cd_{100}	5.02±0.18	4.10±0.10	4.33±0.15	5.01±0.21	5.25±0.094	6.12±0.32
Cr_{10}	0.48±0.033	0.42±0.017	0.25±0.061	0.59±0.023	0.77±0.018	0.95±0.11
Cr_{100}	3.10±0.16	2.51±0.052	2.40±0.071	2.63±0.12	4.11±0.24	4.89±0.25

Note: Cd_{10} and Cd_{100} represent microplastics loaded with Cd from artificial soil solutions at 10 mg/L and 100 mg/L, respectively. Cr_{10} and Cr_{100} represent microplastics loaded with Cr from artificial soil solutions at 10 mg/L and 100 mg/L, respectively.